Fabrication of eco-friendly cellulose - reduced graphene oxide hybrid aerogel from various fruit wastes for water purification

Group 01-20

Yan Jun Jie (4S2-29), Merwin Tham Weng Yahn (4S2-16), Zhang Kai Wen (4S2-32)

Abstract

Oil spills, as well as heavy metal ion and dye pollution, pose significant dangers to the ecosystem and human health. Given the disadvantages in effectiveness, cost, as well as environmental concerns of the current methods of their removal, there is a need for a versatile technology capable of remediating water bodies contaminated by these pollutants. In this study, reduced graphene oxide (rGO), which was synthesised from the peel of the widely-available orange fruit, was added to cellulose extracted from pineapple crown leaves. rGO – cellulose hybrid aerogels were then synthesised, before batch adsorption studies on the removal of copper(II) ions, lead(II) ions and methylene blue dye, as well as an oil sorption test in oil-seawater environment, were performed. Isotherm studies were also conducted to evaluate the hybrid aerogel's maximum adsorption capacity for methylene blue dye. When compared with cellulose aerogels (without rGO), hybrid aerogels were found to be more effective in removing all 3 pollutants. The hybrid aerogel was also found to be reusable in the removal of oil and methylene blue dye for at least 5 and 3 cycles, respectively. The hybrid aerogels synthesised in this study utilised fruit waste in a meaningful way, and also managed to capitalise on the advantages of both rGO and cellulose, enabling it to serve as an eco-friendly, affordable and effective tool for water purification.

1. Introduction

Globally, heavy metal ions, dyes and spilt oil are major pollutants that contaminate water bodies, causing harm to ecosystems and human livelihoods alike.

Heavy metal ions such as copper(II) and lead(II) ions are common water pollutants which are released into water bodies as the by-products of industrial processes. Exposure to copper(II) ions has hepatotoxic and nephrotoxic effects on humans (Shrivastava, 2009), while lead(II) ions can cause severe and irreversible damage to the central nervous system in humans (Harrison & Laxen, 1981). Being non-biodegradable, heavy metal ions ions persist in the environment, posing a continuous threat to flora and fauna, as well as mankind, if not removed. Many different methods of removing heavy metal ions have been documented, such as precipitation by chemical and electrochemical methods. However, the disposal of precipitated wastes is a difficult process. Methods like ion exchange treatment are effective but uneconomical (Dursun & Pala, 2006).

Removing heavy metal ions by adsorption, however, has been widely cited as an efficient method due to its simple operation and lack of secondary pollution. However, many inorganic sorbents such as clays have high costs and low adsorption capacities (Li et al., 2016).

Dyes are another common pollutant which are discharged into water bodies. Around 15% of all dyes produced globally are lost during the dyeing process, causing pollution (Maulin, 2014). The discharge of dyes affects the photosynthetic activities of submerged plants, resulting in adverse effects to the whole ecosystem (Rastogi, Sahu, Meikap, & Biswas, 2008). An example of a dye is methylene blue, a cationic dye heavily used in many industries. Methylene blue releases amines that are toxic and carcinogenic to humans, showing the need for its removal (Pinheiro, Touraud, & Thomas, 2004). However, methylene blue is resistant to degradation by time, so it cannot be efficiently removed in conventional wastewater treatment plants. Therefore, the most effective way of removing methylene blue is through adsorption (Khodaie, Ghasemi, Moradi, & Rahimi, 2013).

A possible solution is reduced graphene oxide (rGO), a quasi-two-dimensional material formed by carbon atoms in the form of sp_2 hybridisation (Zhang, Chen, Bai, & Xie, 2018). It has a large theoretical surface area (Zhang et al., 2014), and many reactive oxygen-containing functional groups, such as hydroxyl, epoxides, and carboxyl groups, which can aid in metal ion complexation through both electrostatic and coordinate bonding (Wang, Sun, Ang, & Tadé, 2013). Furthermore, the conjugated carbon in rGO can attract the aromatic rings of methylene blue through pi-pi interactions. Hence, with these properties, rGO has great potential to be an efficient adsorbent of heavy metal ions and methylene blue dye.

Common methods of synthesising rGO include mechanical exfoliation and chemical vapour deposition, both of which give low yields and are not commercially viable (Compton & Nguyen, 2010). Another option would be to oxidise graphite to form graphene oxide (GO) by Hummer's method – which involves treating graphite with corrosive chemicals such as concentrated sulfuric acid – before reducing the GO to rGO. This procedure emits toxic gases such as nitrogen dioxide, thus posing threats to human health and the environment (Somanathan, Prasad, Ostrikov, Saravanan, & Krishna, 2015). Therefore, an eco-friendly method was proposed in this project. Fruit wastes were carbonised in a furnace with ferrocene (a reducing agent) under atmospheric conditions, forming carbon which was oxidised to form GO and then reduced to yield rGO. This method is straightforward and affordable, and can even provide higher yields of rGO while avoiding the emission of toxic gases.

Orange peels were used in the synthesis of the rGO. Nearly 60 million tonnes of oranges are produced globally per year (Fernandez, Nunell, Bonelli, & Cukierman, 2014). Sadly, orange peels are discarded due to their low economic value into landfills. Thus, using orange peels to synthesise rGO for water purification was environmentally-friendly and meaningful.

Another water pollutant is oil, such as diesel. Oil spills cause significant environmental damage (Nguyen et al., 2014), as well as health problems and long-term changes to the physiology and behaviour of marine animals (Ober, 2010). There are several ways to clean up oil spills, many of which are unviable. Chemical methods such as dispersion are too expensive, while physical methods such as the use of booms and skimmers are ineffective (Duong et al., 2018). On the other hand, absorption is a more economical, efficient and eco-friendly method (Meng et al., 2017). However, some common absorbents like polypropylene have poor reusability, and are not biodegradable (Teas et al., 2001).

Cellulose aerogels may just be the solution to oil spills due to their excellent biodegradability, chemical stability, and low cost of cellulose (Long, Weng & Wang, 2018). Aerogels are the world's lowest-density solid materials, composed of up to 99.98% air by volume (Sehaqui, Zhou & Berglund, 2011), but are still flexible and can even have high absorption capacities of up to 20 times their own weight (Jin, Han, Lin, & Sun, 2015). In this study, cellulose was extracted from pineapple crown leaves. Pineapples are popular tropical fruits, with 16 to 19 million tonnes produced annually. However, the pineapple crown is often discarded due to its low economic value, harming the environment and ecosystems. Therefore, making full use of the pineapple crown is of great practical significance (Dai, Ou, Huang, Liu, & Huang, 2017).

2. Objectives and Hypotheses

The objectives of this study were to fabricate cellulose – rGO hybrid aerogels using fruit wastes; to evaluate the hybrid aerogel's effectiveness in removing oil, heavy metal ions and dye; as well as to determine its reusability in removing dye and oil.

This study hypothesised that the cellulose – rGO hybrid aerogel is more effective than the cellulose aerogel in removing methylene blue dye, copper(II) ions, lead(II) ions, and diesel oil from water; and that cellulose – rGO hybrid aerogels are reusable for at least 3 cycles of sorption.

3. Materials and Methods

3.1. Materials

Methylene blue was purchased from Unichem. Ferrocene was obtained from Sigma-Aldrich. Sodium hydroxide, hydrogen peroxide (6%), copper(II) sulfate pentahydrate, lead(II) nitrate and absolute ethanol were procured from GCE Chemicals. Urea was obtained from

Scharlau and diesel oil was obtained from a local petrol kiosk. Pineapple crown leaves and orange peels were obtained from local fruit stalls.

3.2. Synthesis of Reduced Graphene Oxide (rGO)

Orange peels were washed and dried in an oven at 60 °C overnight until constant mass. They were blended into powder and passed through a sieve to remove larger particles. 0.5 g of the fine powder obtained was mixed with 0.1 g of ferrocene in a crucible and carbonised in a furnace at 300 °C for 20 min under atmospheric conditions. The product was characterised using Scanning Electron Microscopy (SEM), Raman Spectroscopy and X-Ray Diffraction (XRD).

3.3. Synthesis of the aerogels

Pineapple crown leaves were washed, dried in an oven until constant mass and blended. Cellulose was extracted from the dried pineapple crown leaves using a mixture of sodium hydroxide (5% w/v) and hydrogen peroxide (6% v/v) solution per 5 g of dried pineapple crown leaves at a temperature of 55 °C for 2 hours, while stirring vigorously. The extracted cellulose was then washed with deionised water until the pH was neutral, before being dried in an oven until constant mass and ground into finer particles with a blender. The cellulose extracted was characterised by Fourier-transform Infrared Spectroscopy (See Appendix A, page 15) and its morphology was analysed by Scanning Electron Microscopy (SEM). To synthesise cellulose – rGO hybrid aerogels, 2 g of the dried cellulose was dispersed in a urea/sodium hydroxide (10 wt% / 1.9 wt%) solution together with 0.5 g of rGO powder by stirring vigorously for 1 hour, until the mixture was homogeneous. The mixture was then frozen for 24 hours to gelate, using the beaker as a mould. After freezing, the mixture was thawed, before absolute ethanol was added for coagulation for 2 days. The gel was then immersed in deionised water until its pH was neutral, before being pre-freezed at -18 °C for 12 hours and then freeze-dried at -98 °C for 48 hours to yield the aerogel. The morphology of the hybrid aerogel was analysed by SEM. Non-hybrid cellulose aerogels were also synthesised using the same procedure, but without the addition of rGO during dispersion.

3.4. Batch Adsorption Studies

0.1 g of rGO, hybrid and non-hybrid aerogels were each added to 20 ml of a solution containing 50 mg/L of copper(II) ions, lead(II) ions or methylene blue dye in a conical flask and shaken on an orbital shaker for 24 hours at 150 rpm. The supernatant was extracted from each mixture by centrifuging at 13000 rpm for 10 min. The final concentrations of copper(II) and lead(II) ions were measured with a colorimeter (HACH DR 800) and an Atomic Absorption Spectrophotometer (AA 6300 Shimadzu) respectively. For methylene blue, the absorbance of the supernatant at 664.5 nm was measured using a UV-VIS spectrophotometer (Shimadzu UV 1800). The percentage of adsorbate removed from the solution was then calculated with the following formula: $Percentage\ removed = \frac{Initial\ concentration - Final\ concentration}{Initial\ concentration} \times 100\%$

3.5. Isotherm Studies for the Adsorption of Methylene Blue Dye

Batch adsorption was carried out at concentrations of the methylene blue dye solutions from 50 mg/L to 1000 mg/L for the hybrid and non-hybrid aerogels. The equilibrium concentration data was fitted into the Langmuir and Freundlich isotherms (Appendix B, pages 15-17).

3.6. Oil Sorption Test in Oil-Seawater Environment

To prepare artificial seawater, 56.0 g of NaCl, 17.0 g of $MgCl_2$, 8.19 g of $MgSO_4$, 2.50 g of $CaCO_3$ and 2.00 g of KCl were dissolved in 2 litres of deionised water. 10 g of diesel oil was added to a conical flask containing 50 ml of artificial seawater, along with a piece of hybrid or non-hybrid aerogel (0.20 g), before the conical flask was sealed with parafilm. The flask was shaken on an orbital shaker at 150 rpm for 1 hour. The seawater was then separated from the diesel oil using a separating funnel. Hexane was added to extract any remaining diesel in the oil-seawater mixture. Anhydrous sodium sulfate was added to the diesel-hexane mixture to remove any remaining water. A rotary evaporator was used to separate the hexane from the diesel oil. The mass of the remaining oil was monitored over a period of time until constant. The mass of diesel oil absorbed was calculated by subtracting the mass of diesel left in the flask from the initial mass of diesel added (10 g). The following formula was then used to determine the oil sorption capacity: $Q_t = \frac{m_w - m_d}{m_d}$, where Q_t (g/g) is the oil sorption capacity of the aerogel in 60 minutes, m_w (g) is the mass of the aerogel after sorption, and m_d (g) is the mass of the aerogel before sorption.

3.7. Test for the Reusability of the Cellulose – rGO Hybrid Aerogel in Absorbing Oil

The hybrid aerogel was weighed and immersed in 50 ml of diesel oil for 1 hour. Thereafter, it was weighed again and pressed between pieces of tissue paper under 5 kg of brass weights for 30 s to remove the oil absorbed, before being weighed once more. This entire process was repeated for 5 times to determine the reusability of the aerogel. The oil sorption capacity of the aerogel was calculated for each cycle as mentioned under the Oil Sorption Test (Section 3.6).

3.8. Test for the Reusability of the Cellulose – rGO Hybrid Aerogel in Adsorbing Dye

The same procedure as mentioned in the batch adsorption studies was used. After adsorption, the cellulose – rGO hybrid aerogel was filtered out using a sieve and soaked in ethanol to desorb the methylene blue dye. The aerogel pieces were then dried in the oven until constant mass. The concentration of dye remaining in the supernatant was measured and the percentage of pollutants adsorbed was calculated using the formula described in the batch adsorption studies (Section 3.4). The now-dried aerogels were added to another 50 mg/L methylene blue solution and shaken on an orbital shaker. This process was repeated for 3 cycles.

4. Results and Discussion

4.1. Characterisation of rGO by Scanning Electron Microscope (SEM)

The SEM image of the rGO synthesised from orange peel (Figure 1) at 10 µm magnification shows rough, wrinkled and uneven surfaces which contribute to an increased total surface area for adsorption.

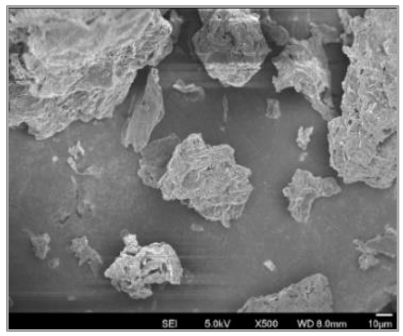

Figure 1. SEM image of the orange peel rGO.

4.2. Characterisation of rGO by Raman Spectroscopy

The Raman spectrum of rGO synthesised from orange peel (Figure 2) displayed 2 bands at 1367 cm$_{-1}$ (D band) and 1585 cm$_{-1}$ (G band) respectively. The G band is associated with the in-plane vibrations of *sp_2* bonded carbon atoms while the D band is due to the out-of-plane vibrations attributed to the presence of structural defects. The peaks are in agreement with rGO synthesised by Khan, Shaur, Khan, Joya, & Awan (2017).

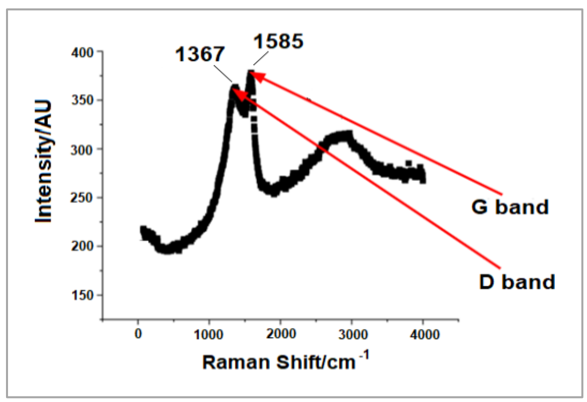

Figure 2. Raman shift of the orange peel rGO.

4.3. Characterisation of rGO by XRD

Characterisation of the orange peel rGO by XRD showed a peak at 24.280°, corresponding to the interlayer distance of 3.63 Å (Figure 3), which was in agreement with rGO synthesised by Stobinski et al. (2014).

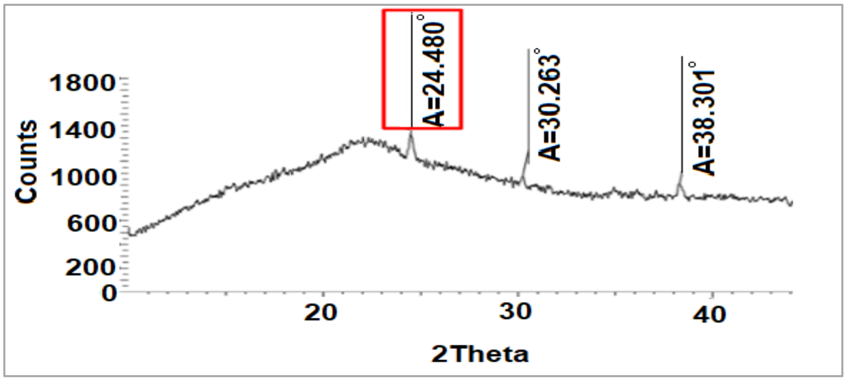

Figure 3. XRD analysis of the orange peel rGO.

4.4. Characterisation of the Cellulose – rGO Hybrid Aerogel by SEM

SEM was used to analyse the structure of the cellulose fibres before and after freeze-drying. After freeze-drying (Figure 5), air spaces could be seen in between the cellulose fibres, suggesting that the aerogel was porous, in contrast to the denser cellulose fibres before freeze-drying was carried out (Figure 4).

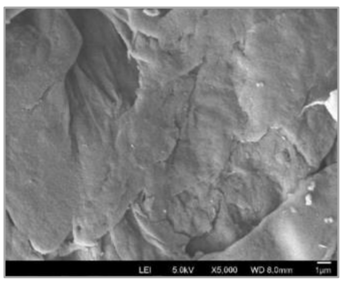

Figure 4. SEM image of the extracted cellulose.

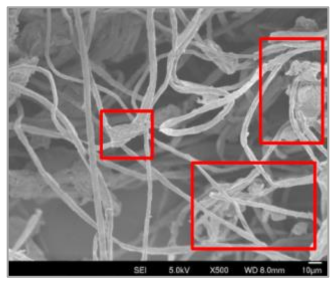

Figure 5. SEM image of the cellulose – rGO hybrid aerogel.

4.5. Batch Adsorption Studies

For rGO, copper(II) and lead(II) ions are adsorbed through the formation of dative bonds with the lone pairs of electrons in the oxygen-containing functional groups of the rGO (Sitko et al., 2013). They are also adsorbed via electrostatic interactions with the negatively charged functional groups, such as carboxylate ions (Figure 6).

The cellulose present in the aerogel contains many hydroxyl functional groups, which are able to adsorb copper(II) and lead(II) ions through the formation of dative bonds (Figure 7).

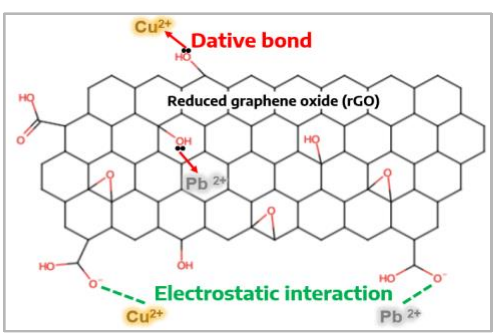

Figure 6. Adsorption mechanism for copper(II) and lead(II) ions onto rGO.

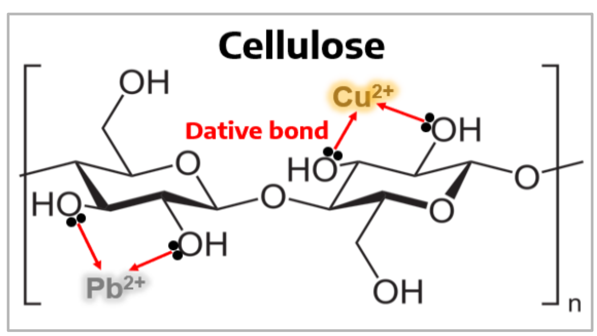

Figure 7. Adsorption mechanism for copper(II) and lead(II) ions onto cellulose.

Figure 8 shows that close to 100% of heavy metal ions were removed by the orange peel rGO. As compared with the cellulose aerogel, the orange peel rGO added during the synthesis of the hybrid aerogel increased the percentage of heavy metal ions removed by it to almost 100%. A Mann Whitney U-Test between the hybrid and cellulose aerogels gave a p-value of 0.00044 (<0.05) for copper(II) ion removal and 0.00058 (<0.05) for lead(II) ion removal, demonstrating a significant difference between the 2 aerogels' percentage removals.

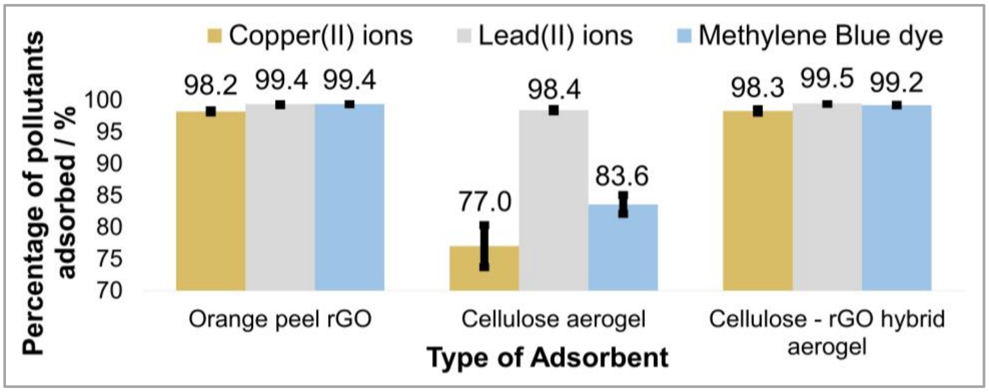

Figure 8. Percentage of heavy metal ions and dye removed by aerogels and orange peel rGO.

However, figure 8 also shows that the cellulose aerogel removed 21.4% more lead(II) ions than copper(II) ions, even without the addition of rGO. Chen and Wang (2007) found through a linear regression analysis that a higher covalent index of a metal ion was correlated with a higher maximum adsorption capacity, q_{max} of an adsorbent. The lead(II) ion has a covalent index of 6.41 while that of the copper(II) ion is 2.64 (Wang, Pan, Cai, Guo, & Xiao, 2017), meaning that the lead(II) ion has a stronger attraction to the lone pair of electrons in the oxygen-containing functional groups of cellulose, allowing more of it to be adsorbed.

Methylene blue dye is adsorbed through pi-pi interactions between the conjugated carbon in rGO with the dye's aromatic rings. The oxygen-containing functional groups on the rGO also adsorbs the dye via electrostatic interactions and hydrogen bonds (Figure 9) (Minitha, Lalitha, Jeyachandran, Senthilkumar, & Rajendra Kumar, 2017). Cellulose is also able to adsorb methylene blue dye through the formation of hydrogen bonds, but the addition of rGO for the hybrid aerogel increases the percentage removal significantly (Figure 8).

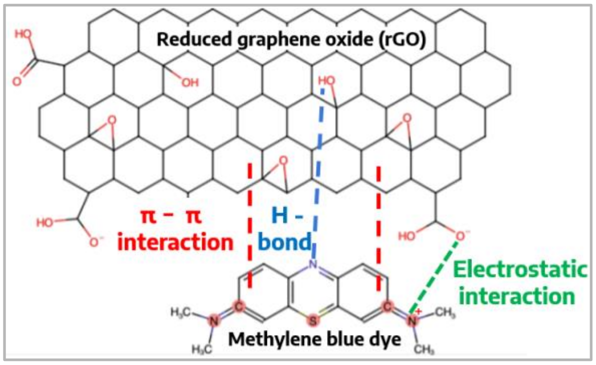

Figure 9. Adsorption mechanism for methylene blue dye onto rGO.

4.6. Isotherm Studies for the Adsorption of Methylene Blue Dye

The equilibrium concentration data for both the hybrid and non-hybrid aerogels was fitted into the Langmuir and Freundlich isotherms (Appendix B, pages 15-17). The Langmuir isotherm is a better fit for both aerogels, suggesting that the adsorption is monolayer. The maximum adsorption capacities of both aerogels were derived from the gradient of the equations obtained from the Langmuir isotherm (Table 1). The hybrid aerogel has a higher maximum adsorption capacity than the non-hybrid aerogel due to the addition of rGO during its synthesis.

Table 1. Maximum adsorption capacities of aerogels on methylene blue dye.

Type of Adsorbent	Maximum Adsorption Capacity / mg g^{-1}	Reference
Non-hybrid cellulose aerogel	71.9	This study
Cellulose – rGO hybrid aerogel	105.0	This study

4.7. Oil Sorption Test in Oil-Seawater Environment

The porous networks of cellulose in the aerogels allow them to absorb diesel. Figure 10 shows that hybrid aerogels have significantly higher sorption capacities than non-hybrid aerogels (P-value of Mann Whitney = 0.017), which can be attributed to the non-polar conjugated carbon in rGO interacting with the diesel via dispersion forces, thus increasing the amount of diesel absorbed. The hybrid aerogel also outperformed milkweed fibre, another common oil sorbent, which has an oil sorption capacity of 7.3 g/g (Karan, Rengasamy, & Das, 2011).

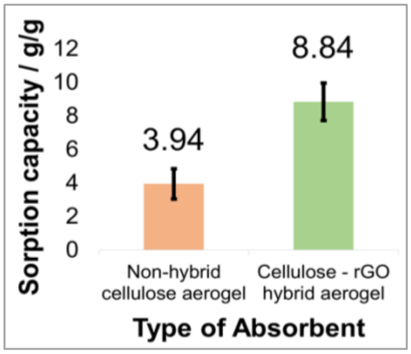

Figure 10. Sorption capacities of aerogels in oil-seawater environment.

4.8. Test for the Reusability of the Cellulose – rGO Hybrid Aerogel in Absorbing Oil

Figure 11 shows that after the first cycle, there is a general decreasing trend in the aerogel's sorption capacity, which could be due to the aerogel structures collapsing under the pressure exerted by the brass weights, causing it to become denser and less porous, thus decreasing the mass of oil that it could absorb. However, the insignificant differences (P-value of Kruskal-Wallis test = 0.18) between the sorption capacities from cycle 2 onwards suggests that the aerogel has the potential to be continuously reused.

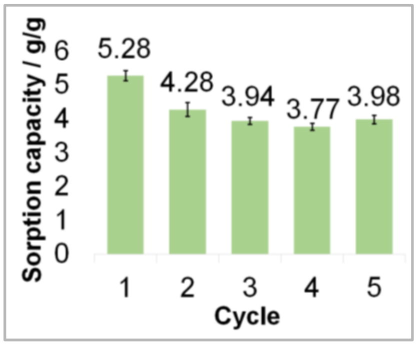

Figure 11. Reusability of the hybrid aerogel in absorbing oil.

4.9. Reusability of the Cellulose – rGO Hybrid Aerogel in Adsorbing Dye

Overall, there is a decrease in the percentage of methylene blue dye adsorbed (Figure 12) from the 1st to the 3rd adsorption cycle, which may be attributed to the incomplete desorption of the dye from the aerogel. Another possibility could be the loss of rGO from the surface of the aerogel during the desorption process. However, a high percentage of dye adsorbed was still maintained throughout the 3 cycles, suggesting that the hybrid aerogel is reusable.

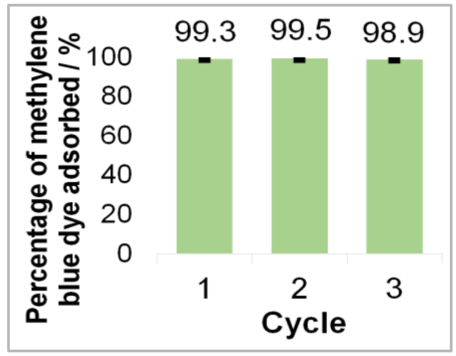

Figure 12. Reusability of the cellulose – rGO hybrid aerogel in adsorbing dye.

5. Conclusions and Recommendations for future work

Cellulose – rGO hybrid aerogels were successfully synthesised from pineapple crowns and orange peels. This method of synthesising aerogels allowed food waste to be utilised in a meaningful way, reducing waste. Synthesising rGO by the carbonisation of fruit peels with ferrocene is a straightforward, safe and scalable process that avoids the health risks and environmental hazards associated with the toxic fumes produced as a by-product of Hummer's Method. Using the cellulose – rGO hybrid aerogel was also an eco-friendlier way of tackling the problem of oil spills, rather than commonly-used petroleum-derived sorbents such as polypropylene.

The rGO present in the hybrid aerogel enhances its oil sorption capacity, and improves the percentage removal of copper(II) ions, lead(II) ions and methylene blue dye, as compared to non-hybrid cellulose aerogels. For both aerogels, the Langmuir Isotherm is a better fit, suggesting that the adsorption of methylene blue dye is monolayer. With the addition of rGO, the maximum adsorption capacity of the aerogel on methylene blue increases by about 1.5 times. Furthermore, the hybrid aerogel is also reusable in the sorption of diesel oil and dye. These characteristics enable the hybrid aerogel to function as an eco-friendly, versatile and effective tool for water purification.

In future, isotherm studies can be extended to the adsorption of heavy metal ions. Oil sorption tests can be conducted on other types of oil, such as motor oil. The scope of the current study can also be extended to other pollutants such as anionic dyes, organic solvents, pesticides and pharmaceuticals. Finally, thermodynamic and kinetic studies can also be conducted to gain further insight into the adsorption mechanisms of the hybrid aerogel.

References

Chen, C., & Wang, J. (2007). Influence of metal ionic characteristics on their biosorption capacity by Saccharomyces cerevisiae. *Applied Microbiology and Biotechnology, 74,* 911-917. DOI: 10.1007/s00253-006-0739-1

Compton, O.C., & Nguyen, S.T. (2010). Graphene Oxide, Highly Reduced Graphene Oxide, and Graphene: Versatile Building Blocks for Carbon-Based Materials. *Small, 6(6),* 711–723. DOI: 10.1002/smll.200901934

Dai, H., Ou, S., Huang, Y., Liu, Z., & Huang, H. (2017). Enhanced swelling and multiple-responsive properties of gelatin/sodium alginate hydrogels by the addition of carboxymethyl cellulose isolated from pineapple peel. *Cellulose*, *25(1),* 593-606. DOI: 10.1007/s10570-017-1557-6

Duong, H.M., Liu, P., Nguyen, T.X., Nguyen, S.T., Feng, J., & Cheng, H. (2018). Cellulose and Protein Aerogels for Oil Spill Cleaning, Life Science and Food Engineering Applications. *Green Chemistry Series Biobased Aerogels*, *14,* 228-260. DOI: 10.1039/9781782629979-00228

Dursun, S., & Pala, A. (2006). Lead pollution removal from water using a natural zeolite. *J. Int. Environmental Application & Science, 2,* 11-19. Retrieved from http://www.jieas.com/fvolumes/vol071-2/2-1&2-3.pdf

Fan, M., Dai, D., & Huang, B. (2012). Fourier Transform Infrared Spectroscopy for Natural Fibres. *Fourier Transform - Materials Analysis.* ISBN: 978-953-51-0594-7

Fernandez, M.E., Nunell, G.V., Bonelli, P.R., & Cukierman, A.L. (2014). Activated carbon developed from orange peels: Batch and dynamic competitive adsorption of basic dyes. *Industrial Crops and Products, 62,* 437–445. DOI: 10.1016/j.indcrop.2014.09.015

Harrison, R.M., & Laxen, D.P.H. (1981). Lead Pollution: Causes and Control. *Springer Nature.* DOI: 10.1007/978-94-009-5830-2

Jin, C., Han, S., Lin, J., & Sun, Q. (2015). Fabrication of cellulose-based aerogels from waste newspaper without any pretreatment and their use for absorbents. *Carbohydrate Polymers, 123,* 150–156. DOI: 10.1016/j.carbpol.2015.01.056.

Karan, P.C., Rengasamy, R.S., & Das, D. (2011). Oil Spill Cleanup by Structured Fibre Assembly. *Indian Journal of Fibre and Textile Research*, *36,* 190-200. Retrieved from https://pdfs.semanticscholar.org/d794/9bb668411ea5d77e76c18266ea578f69e6bd.pdf

Khan, Q.A., Shaur, A., Khan, T.A., Joya, Y.F., & Awan, M.S. (2017). Characterization of reduced graphene oxide produced through a modified Hoffman method. *Cogent Chemistry, 3,* 1298980. Retrieved from https://www.cogentoa.com/article/10.1080/23312009.2017.1298980.pdf

Khodaie, M., Ghasemi, N., Moradi, B., & Rahimi, M. (2013). Removal of Methylene Blue from Wastewater by Adsorption onto $ZnCl_2$ Activated Corn Husk Carbon Equilibrium Studies. *Journal of Chemistry,* 1–6*.* DOI: 10.1155/2013/383985

Li, A., Lin, R., Lin, C., He, B., Zheng, T., Lu, L., & Cao, Y. (2016). An environment-friendly and multi-functional absorbent from chitosan for organic pollutants and heavy metal ion. *Carbohydrate Polymers, 148,* 272–280. DOI: 10.1016/j.carbpol.2016.04.070

Long, L.Y., Weng, Y.X., & Wang, Y.Z. (2018). Cellulose Aerogels: Synthesis, Applications, and Prospects. *Polymers, 10(6),* 623. Retrieved from https://doi.org/10.3390/polym10060623

Maulin, P.S. (2014). On Site Application of Pseudomonas Aeruginosa ETL-1942 and Bacillus Cereus ETL-1949 in Decolorization and Degradation of Remazol Black-B. *International Journal of Environmental Bioremediation & Biodegradation, 2(3),* 139-145. DOI: 10.12691/ijebb-2-3-7

Meng, G., Peng, H., Wu, J., Wang, Y., Wang, H., Liu, Z., & Guo, X. (2017). Fabrication of superhydrophobic cellulose/chitosan composite aerogel for oil/water separation. *Fibers and Polymers*, *18(4),* 706-712. DOI: 10.1007/s12221-017-1099-4

Minitha, C.R., Lalitha, M., Jeyachandran, Y.L., Senthilkumar, L., & Rajendra Kumar, R.T. (2017). Adsorption behaviour of reduced graphene oxide towards cationic and anionic dyes: Co-action of electrostatic and π – π interactions. *Materials Chemistry and Physics, 194,* 243–252. DOI: 10.1016/j.matchemphys.2017.03.048

Nguyen, S.T., Feng, J., Ng, S.K., Wong, J.P., Tan, V.B., & Duong, H.M. (2014). Advanced thermal insulation and absorption properties of recycled cellulose aerogels. *Colloids and Surfaces A: Physicochemical and Engineering Aspects, 445,* 128-134. Retrieved from https://doi.org/10.1016/j.colsurfa.2014.01.015

Ober, H.K. (2010). Effects of Oil Spills on Marine and Coastal Wildlife. *UF/IFAS North Florida Research and Education Center.* Retrieved from http://edis.ifas.ufl.edu/uw330

Pinheiro, H.M., Touraud, E., & Thomas, O. (2004). Aromatic amines from azo dye reduction: status review with emphasis on direct UV spectrophotometric detection in textile industry wastewaters. *Dyes and Pigments, 61(2),* 121–139. DOI: 10.1016/j.dyepig.2003.10.009

Rastogi, K., Sahu, J.N., Meikap, B.C., & Biswas, M.N. (2008). Removal of methylene blue from wastewater using fly ash as an adsorbent by hydrocyclone. *Journal of Hazardous Materials, 158(2-3),* 531–540. DOI: 10.1016/j.jhazmat.2008.01.105

Sehaqui, H., Zhou, Q., & Berglund, L.A. (2011). High-porosity aerogels of high specific surface area prepared from nanofibrillated cellulose (NFC). *Composites Science and Technology, 71,* 1593-1599. DOI: 10.1016/j.compscitech.2011.07.003

Shrivastava, A.K. (2009). A Review of Copper Pollution and its Removal from Water Bodies by Pollution Control Technologies. *Indian Journal of Environmental Protection, 29(6),* 552-560. Retrieved from
http://www.indiaenvironmentportal.org.in/files/A%20review%20on%20copper%20pollution.pdf

Sitko, R., Turek, E., Zawisza, B., Malicka, E., Talik, E., Heimann, J., ... Wrzalik, R. (2013). Adsorption of divalent metal ions from aqueous solutions using graphene oxide. *Dalton Transactions*, *42(16),* 5682. DOI: 10.1039/c3dt33097d

Somanathan, T., Prasad, K., Ostrikov, K., Saravanan, A., & Krishna, V.M. (2015). Graphene Oxide Synthesis from Agro Waste. *Nanomaterials, 5,* 826-834. DOI: 10.3390/nano5020826

Stobinski, L., Lesiak, B., Malolepszy, A., Mazurkiewicz, M., Mierzwa, B., Zemek, J., … Bieloshapka, I. (2014). Graphene oxide and reduced graphene oxide studied by the XRD, TEM and electron spectroscopy methods. *Journal of Electron Spectroscopy and Related Phenomena, 195,* 145–154. DOI: 10.1016/j.elspec.2014.07.003

Teas, C., Kalligeros, S., Zanikos, F., Stournas, S., Lois, E., & Anastopoulos, G. (2001). Investigation of the effectiveness of absorbent materials in oil spills clean up. *Desalination, 140,* 259–264. DOI: 10.1016/S0011-9164(01)00375-7

Wang, F., Pan, Y., Cai, P., Guo, T., & Xiao, H. (2017). Single and binary adsorption of heavy metal ions from aqueous solutions using sugarcane cellulose-based adsorbent. *Bioresource Technology, 241,* 482–490. DOI: 10.1016/j.biortech.2017.05.162

Wang, S., Sun, H., Ang, H.M., & Tadé, M.O. (2013). Adsorptive remediation of environmental pollutants using novel graphene-based nanomaterials. *Chemical Engineering Journal, 226,* 336–347. DOI: 10.1016/j.cej.2013.04.070

Zhang, C.Z., Chen, B., Bai, Y., & Xie, J. (2018). A new functionalized reduced graphene oxide adsorbent for removing heavy metal ions in water via coordination and ion exchange. *Separation Science and Technology,* 1–10. DOI: 10.1080/01496395.2018.1497655

Zhang, Y., Yan, L., Xu, W., Guo, X., Cui, L., Gao, L., ... Du, B. (2014). Adsorption of Pb(II) and Hg(II) from aqueous solution using magnetic $CoFe_2O_4$-reduced graphene oxide. *Journal of Molecular Liquids, 191,* 177–182. DOI: 10.1016/j.molliq.2013.12.015

Appendix A

Characterisation of the pineapple cellulose by FTIR

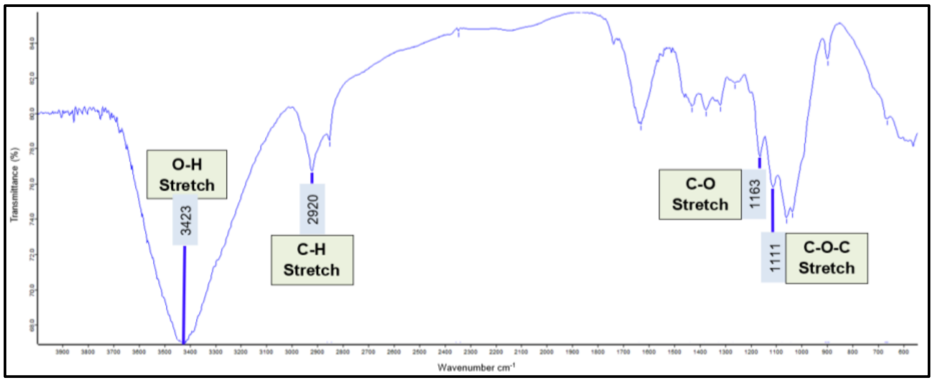

Figure 13. FTIR spectrum of cellulose extracted from pineapple waste.

FTIR was used to analyse the structure of the pineapple cellulose. The FTIR spectrum (Figure 13) reveals peaks corresponding to functional groups characteristic of cellulose, including the O-H stretch (3423 cm^{-1}), C-H stretch (2920 cm^{-1}), C-O stretch (1163 cm^{-1}) as well as the C-O-C stretch (1111 cm^{-1}), which were in agreement with cellulose extracted by Fan, Dai and Huang (2012).

Appendix B

Adsorption Isotherms of non-hybrid cellulose aerogel & cellulose – rGO hybrid aerogel

The equilibrium concentration data obtained from adsorption isotherm studies on methylene blue dye were fitted into the Langmuir and Freundlich isotherms.

The Langmuir isotherm assumes that the adsorbate is adsorbed over a uniform adsorbent surface at a constant temperature. The linear form of the Langmuir isotherm equation is given by:

$$\frac{C_e}{q_e} = \frac{1}{bq_m} + \frac{C_e}{q_m}$$

Where C_e is the equilibrium concentration of methylene blue (mg/L), q_e is the equilibrium capacity of the adsorbents (mg/g), b is the Langmuir constant that indicates the sorption intensity and q_m is the maximum adsorption capacity (mg/g).

The Freundlich isotherm assumes that the adsorption occurs on a heterogeneous surface. The linear form of the Freundlich isotherm equation is given by:

$$\log(Q_e) = \log(K_F) + \frac{1}{n}\log(C_e)$$

Where C_e is the equilibrium concentration of methylene blue (mg/L), q_e is the equilibrium capacity of the adsorbents (mg/g), K_F is a constant related to sorption capacity and n corresponds to sorption intensity.

The Langmuir and Freundlich isotherm plots are shown below:

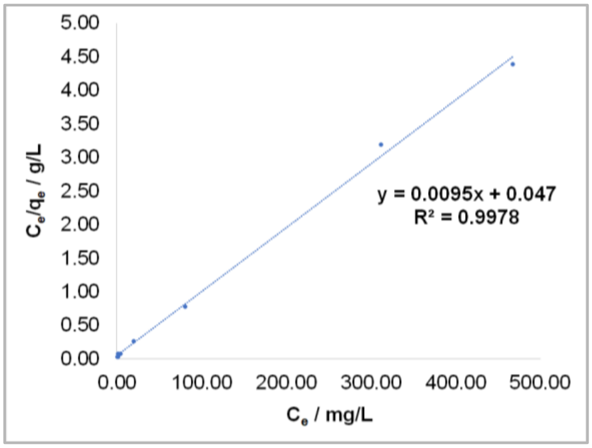

Figure 14. Langmuir isotherm for the cellulose – rGO hybrid aerogel.

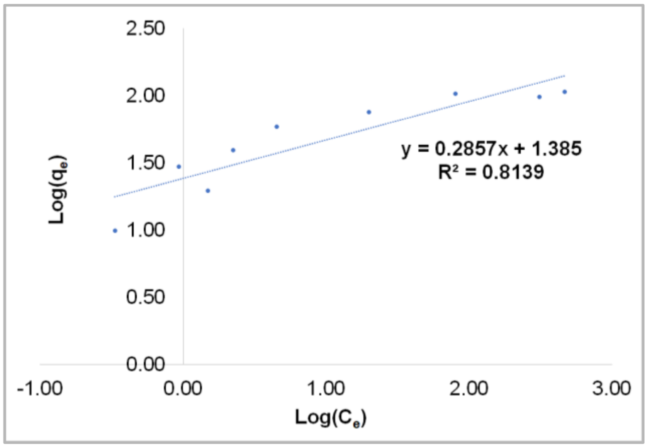

Figure 15. Freundlich isotherm for the cellulose – rGO hybrid aerogel.

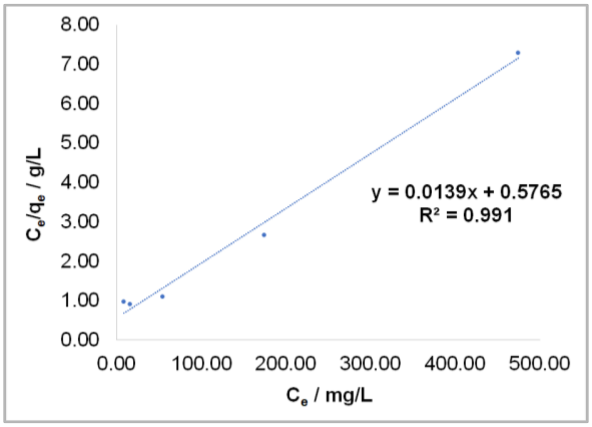

Figure 16. Langmuir isotherm for the non-hybrid cellulose aerogel.

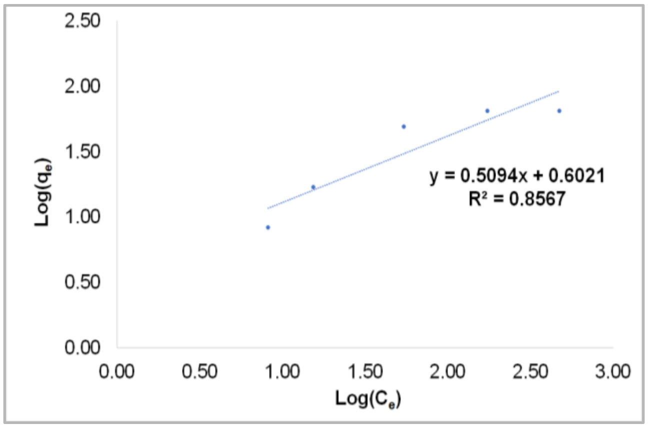

Figure 17. Freundlich isotherm for the non-hybrid cellulose aerogel.

The value of q_m was computed from the gradient of the Langmuir isotherm plot of C_e/q_e versus C_e. Similarly, the value of n was computed from the gradient of the Freundlich plot of $\log(q_e)$ versus $\log(C_e)$. The isotherm parameters obtained are summarised in table 2.

Table 2: Isotherm parameters for the non-hybrid cellulose aerogel & cellulose – rGO hybrid aerogels.

	Langmuir isotherm parameters		**Freundlich isotherm parameters**	
	q_m (mg/g)	R_2	n	R_2
Non-hybrid cellulose aerogel	71.9	0.998	3.50	0.814
Cellulose – rGO hybrid aerogel	105.0	0.991	1.96	0.857

Comparison of the coefficient of determination (R_2) of the linearised forms of both isotherms suggests that the Langmuir model yields a better fit for the equilibrium adsorption data of methylene blue dye onto both aerogels. The maximum adsorption capacity, q_m, of the hybrid aerogel was higher than that of the non-hybrid aerogel.